Nuclear Inst. and Methods in Physics Research B 465 (2020) 73–78

Contents lists available at ScienceDirect

Nuclear Inst. and Methods in Physics Research B

journal homepage: www.elsevier.com/locate/nimb

Positron annihilation studies of long range effect in Ar, N and C ion-implanted silicon

K. Siemek[a,b,*], J. Dryzek[b], M. Mitura-Nowak[b], A. Lomygin[c], M. Schabikowski[b]

[a] Joint Institute for Nuclear Research, 141980 Dubna, Russian Federation
[b] Institute of Nuclear Physics, PAS, 31-342 Kraków, Poland
[c] National Research Tomsk Polytechnic University, Lenin Avenue 30, 634050 Tomsk, Russian Federation

ARTICLE INFO

Keywords:
Positron anihilation spectroscopy
Defects
Ion implantation

ABSTRACT

The thermal evolution of defects inside and beyond the implantation layer in Si wafer exposed to the irradiation with 25 keV C^+, N^+ and Ar^+ ions with different doses has been investigated by positron beam measurements. Two types of defects were detected: the small cavities and divacancies in the implanted layer which thickness corresponding to the projectile range. Cavities were only present for dose $2*10^{16}$ and were not observed for $2*10^{14}$ and $2*10^{15}$ ions/cm^2. For the dose of $2*10^{16}$ ions/cm^2 the defects were detected also beyond the implantation layer indicating the presence of the long range effect. Obtained results indicate on influence of ion type and dose on defect distribution and its thermal evolution beyond the implanted layer. The recovery process was similar for Ar^+ and N^+ but differ for C^+ ion implantation.

1. Introduction

The ion implantation is commonly used for subsurface modifications, especially useful for doping semiconductors in planar technology. In a simple way, one can localize different ions at different depths from the entrance surface and change, for instance, electronic properties in the implanted layer (IL). Even at high doses of 10^{17} ions/cm^2 C^+ and N^+ ions, chemical reactions can occur and thin layers of SiC and SiN can be formed [1,2]. At medium fluencies, mainly generation of point defects like interstitial atoms determine the final properties, for instance, C-atoms are responsible for G-centre emission used in silicon photonics [3] and N are used for selective oxidation purposes [1]. Also, the presence of buried cavities obtained during annealing of IL can be used to utilize the metallic impurities and improve electrical properties of Si [4].

Swift ions interacting with target atoms losing energy during ionization and collisions [5]. However, during these many damages ranging from point defects to phase transitions are being generated. They arise as a result of inelastic nuclear collisions, but also ionization induces a local temperature increase in the spike region. These defects exhibit a certain depth distribution that can be simulated using the SRIM/TRIM code [6]. But only scattering processes are considered, other processes that accompany defects are neglected. Initial defects created during ion implantation is composed from vacancies, interstitials and IV pairs. When its number increase it could agglomerate and form bigger structural defects. Higher doses, energies and lower target temperature promote formation of larger vacancy clusters and could also cause amorphization [7,8]. The large vacancy clusters can collapse and dislocation loops can occur. High mobility of Si single vacancy at room temperature lead to changes of initial defect profile [9]. Most of them disappear in recombination process, others cluster and form more stable agglomerates. Shi et al. [10] calculated that only 5–25% of initial defects remain in Si after neutron irradiation. The presence of voids, amorphous region and interstitials also cause appearance of stress, rarely considered in defects calculations. Above reasons indicate that defects distribution should be obtained on experimental way. Defects are located not only in the IL, which thickness equals to the projectile range of implanted ion, some studies indicate that defects are extended beyond this layer. This phenomena is called in the literature as long range effect (LRE) [11]. The recent studies performed in pure metals: Ag [12,13], Fe [13], Cu [14] and Ti [15] irradiated with swift Xe^{26+} heavy ion indicate that the thickness of the extended damage layer is comparable with the projectile range however, it can depend on the dose and materials properties because no LRE was observed in pure Au [16]. The nature of the LRE still is not clear enough, in Ref. [13], the authors concluded that its origin is the stress distribution, which exceeds the yield strength in the IL and induces plastic deformation beyond. The question arises how this effect depend on the type of ion and dose for light ion implantation to typical semiconductors. In silicon implanted with light ion extended zones of defects was noted during

* Corresponding author.
E-mail address: siemek.krzysztof@gmail.com (K. Siemek).

https://doi.org/10.1016/j.nimb.2019.12.026
Received 18 November 2019; Accepted 27 December 2019

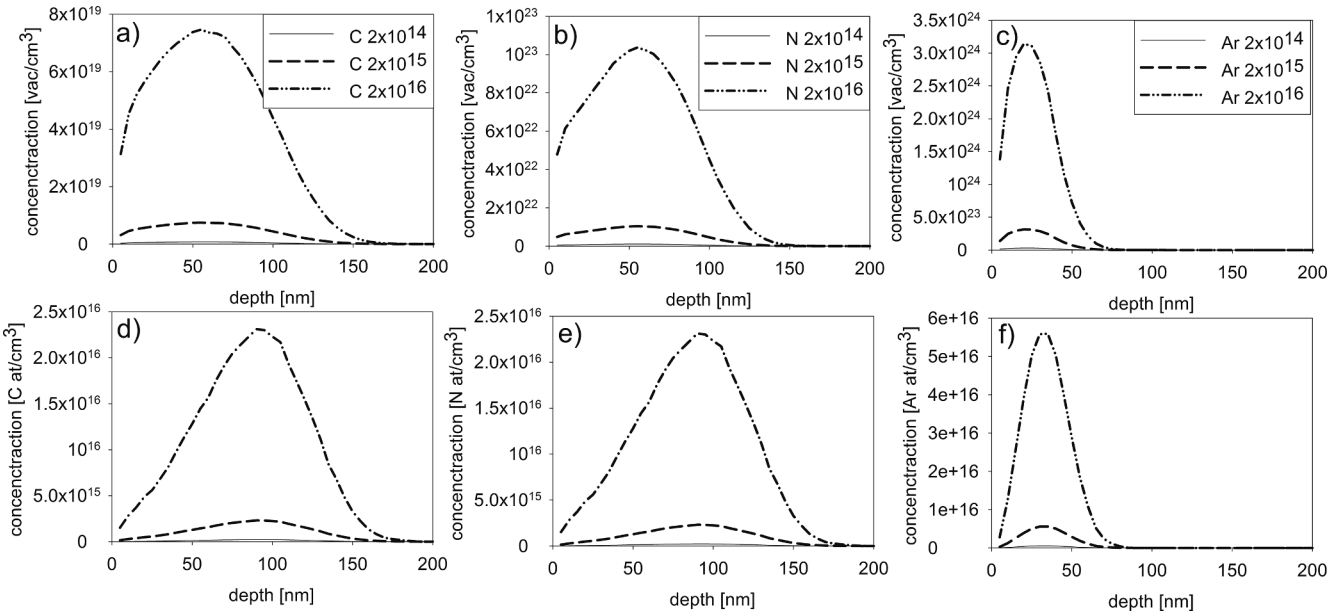

Fig. 1. The depth distributions of vacancies a-c) and ions d-f) obtained using software TRIM [6] for Si samples implanted with carbon, nitrogen and argon ions with energy 25 keV and doses 2×10^{14}, 2×10^{15}, 2×10^{16} ions/cm^2.

As^+, P^+, O^-, Ar^+-implantation [17–19], but not observed for 100 keV H^+ [17] or 50–150 keV B^+ [20] ions. Also dependency of ion dose on damaged area size was reported [19–21]. Understanding of defect behavior in the extended damage layer can important for future devices in Si industry.

During thermal treatment used to decrease number of defects and activate dopants the defects distribution changes. A numerous of works are focused on defects structural studies during annealing [2,7,17–19,22,23]. They indicate that damaged region recovery in different temperature caused by presence of hierarchical types of defects. Most stable of them predominantly disappear at temperature 800–1000 °C. However, it should be noted that presence of dopants atoms and impurities could strongly affect the annealing process, i.e. Fujinami et al. [22] report vacancy-oxygen V-O complexes stables even after annealing in 1350 °C. The different V-N and V-C complexes were observed during annealing of carbon and nitrogen implanted Si [2,23]. Presence of these complex should influence on annealing of defects inside the IL. However, its impact beyond is still unknown and worth investigations.

A typical techniques used to study implantation damages are TEM, Raman spectroscopy, infrared spectroscopy, Rutheford backscaterring, double crystal diffractometry, and electron spin resonance. Among this methods, in last decades very promising technique to study of open volume defects and voids appear i.e. positron annihilation spectroscopy (PAS). Depending on positron incident energies PAS allows one to study subsurface zone ranging from nanometers up to few μm without destruction of sample. A variable energy positrons beam (VEP) can be used to determine depth distribution of vacancies after ion implantation and observe its concentration changes during annealing.

In current studies, we intend to use VEP technique to study the Si wafer samples irradiated with C^+, N^+, and Ar^+ ions with 25 keV incident energy and different doses ranging from 2×10^{14} to 2×10^{16}. The range of incident positrons, in this case of about a few of micrometers, is higher than the projectile range of ions, then we will be able to detect defects in the IL and beyond it. The samples will be annealed in order to observe the evolution of these defects under temperature. The most of investigations was performed using VEP, but the works also include partial ion distribution studies using glow-discharge optical emission spectroscopy for carbon irradiated samples.

2. Experimental

Samples were prepared from single-crystal silicon wafer with orientation of (1 0 0). The dimensions of the samples were $10 \times 10 \times 1$ mm. Pre-cleaned wafers were implanted with 25 keV energy Ar^+, N^+ and C^+ ions with fluencies of 2×10^{14}, 2×10^{15}, 2×10^{16} ions per cm^2. The ion implantation was performed at room temperature on dual beam ion implanter in the Henryk Niewodniczanski Institute of Nuclear Physics, Krakow, Poland. Typical ion beam current was about 1μA.

Slow positron beam experiment VEP was performed at JINR in Dubna, Russia. The energy of incident positrons was ranged between 0.1 and 35 keV, which correspond to studied depth up to 4.6 μm. The beam intensity was about 10^5 e^+/s and its diameter was 5 mm. The HPGe detector ORTEC GEM25P4-70 with an energy resolution (FWHM) of 1.20 keV at 511 keV was used to monitor an annihilation line shape parameters. The S and W parameters are defined as a ratio of the area below the central or wing part, respectively, of the annihilation line to the total area marked by the peak. The S parameter value reflects the fraction of positron annihilation with low momentum electrons mainly present in defects. Thermal annealing of the samples was performed under vacuum condition 10^{-3} Pa during period of 1 h in temperature range from 500 °C to 900 °C. After annealing samples was slowly cold down to the room temperature. On such samples the VEP measurements at room temperature were performed.

Two samples implanted with C^+ ions with lowest and medium dose was also measured using Glow Discharge Optical Emission Spectroscopy (GDOES) using GD - Profiler 2. In case of the other samples implanted with N^+ and Ar^+ due to presence of this elements in GDOES chamber the ion distributions were not determined.

3. Result and discussion

The implanted atoms and generated vacancies concentration after implantation was simulated using TRIM [6], and are presented on Fig. 1. For C^+ and N^+ ion with 25 keV the projectile range is equal to 170 nm and maximum is reached at 95 nm, Fig. 1. Heavier Ar^+ ions are stopped at shallower depth, the highest value correspond to 35 nm and ions could reach only of 70 nm. In the simulated vacancies concentration profiles which not include recombination and diffusion process

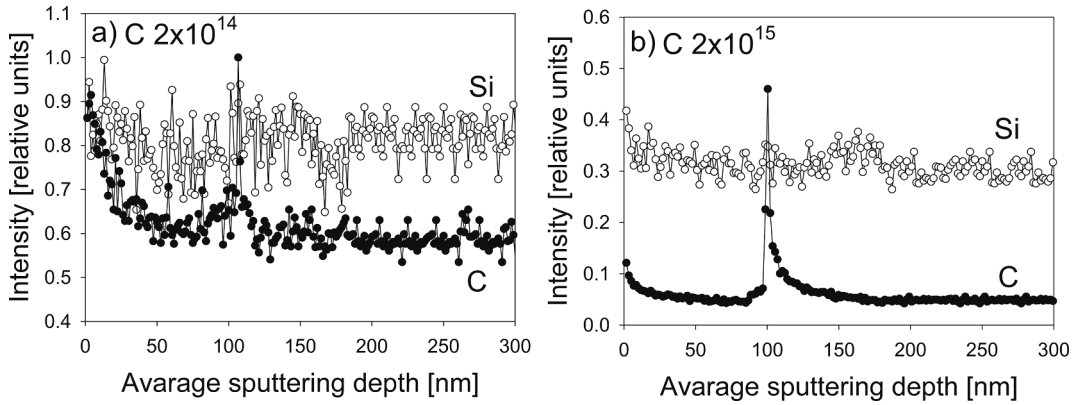

Fig. 2. The Si and C distributions obtained using GDOES method for Si samples implanted with carbon ions with energy 25 keV and doses 2×10^{14}, 2×10^{15} ions/cm^2.

maximum is observed at the depth of 50 nm for C^+, N^+ and 25 nm for Ar^+, respectively. Experimental distribution of C atom in the implanted samples obtained using GDOES technique is shown in Fig. 2. The highest concentration of C atoms occurs at the depth around 100 nm and it corresponds well to simulated ones, this indicates on absence channeling effect of C ions. However, obtained shape of profiles differ from simulated, Fig. 1.

The VEP experiments allow one to get information about the changes of defect concentration below the entrance surface. However, implanted positrons have a certain depth distribution, it is generally accepted that this distribution is represented by the Makhovian function [24], where the positron mean implantation depth $\bar{z}$ can be estimated as:

$$\bar{z} = \frac{A}{\rho} E^n \tag{1}$$

where E is positron implantation energy in keV, ρ is mass density of Si 2.33 g/cm^3, $A = 2.48$ μgcm^{-2}keV^{-n} and $n = 1.729$ are parameters obtained from the Monte Carlo simulation [24]. In Fig. 3 the dependency of the S-parameters measured for the different positron incident energies for all Si samples after ions implantation is presented. On the top axis the mean positron implantation depth, according Eq. (1) is added.

As expected, the ion implantation changes the S-parameter dependencies, Fig. 3. Before irradiation, in the reference sample S-parameter slowly increase and at the depth around 1 μm saturate with value about 0.483 which is a bulk value, closed circles in Fig. 3. This increment is caused by positron diffusion to the surface where annihilation also takes place, at the surface the S-parameter has a lower value than in the interior. After irradiation the S-parameter in all cases drastically increase indicating on presence of defects especially in the IL. The maximum of the dependency is reached at depth corresponding well with TRIM simulation from Fig. 1, and then it slowly decrease reaching bulk value present already for the reference sample. The obtained dependencies can be described theoretically, this description must include the initial positron implantation profile and their diffusion, all these issues were incorporated in the VEPFIT code [26]. Using this code in the fitting procedure we can obtain, as the adjustable parameters: the value of the S-parameter, positron diffusion length in the selected layers and their thickness. Number of these layers is assumed in the applied model in the fitting procedure. The solid lines in Fig. 3 presents the best fits obtained using VEPFIT code. For reference sample the obtained diffusion length L_+ was equal to 230 nm and correspond well to value 245 nm for defect free Si [22,25]. The S-parameter dependency strongly depends on the irradiation dose. Let's consider first the doses: $2*10^{14}$ and $2*10^{15}$ ions/cm^2, where the differences in the dependencies are quite small. In this cases two layers fitting model was assumed. The first layer represent the damage layer which thickness is the adjustable parameter, and the second one undamaged layer located beyond. The thickness, S-parameter and L_+ values in this layer were fitted and the obtained values are gathered in Table 1. The small increment of S-parameters for the higher dose was noted for all samples. The positron diffusion length value decreases when the higher dose was applied, except for samples irradiated with Ar ions. The damaged layer thickness increases for N^+ and Ar^+ implanted samples, but it decrease for C^+ ions. This is surprising, it can be supposed that the concentration of defects and size of the damaged layer will increase or stay at the same level. Also anyone could expect shortening of L_+ corresponding to increased defect number. However, L_+ remain almost constant for N^+

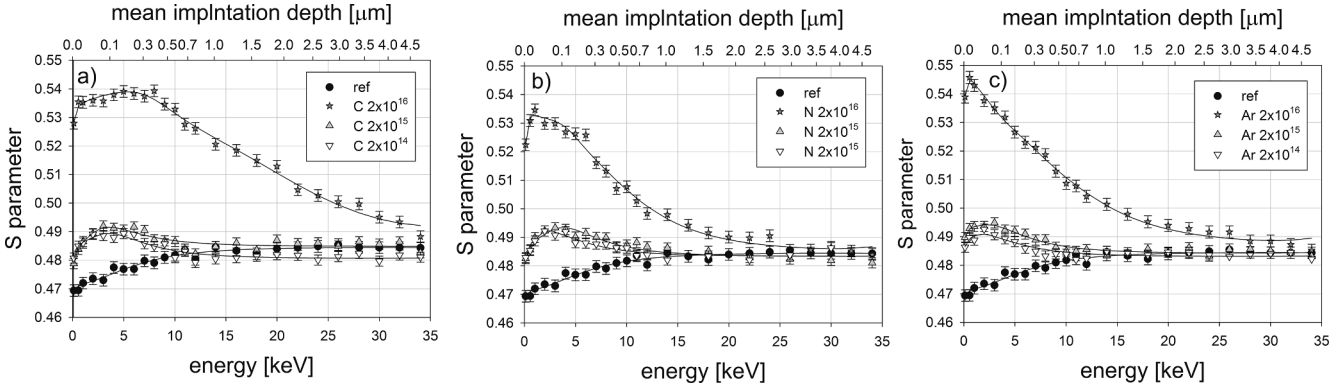

Fig. 3. The S-parameter in function of incident positron energy for Si samples implanted with C^+ a), N^+ b) and Ar^+ c) ions with energy 25 keV and doses 2×10^{14}, 2×10^{15}, 2×10^{16} ions/cm^2. The upper axis correspond to mean implantation depth of positron calculated according Eq. (1). The solid lines represent the best fit obtained using VEPFIT code. The values of adjustable parameter obtained from the VEPFIT code are gathered in Table 1.

Table 1
The values of the adjustable parameters obtained from VEPFIT code, in the damage layer (see Fig. 3) for Si samples implanted with C^+, N^+ and Ar^+ ions with energy 25 keV and doses $2x10^{14}$, 2×10^{15} ions/cm^2.

Sample	S-parameter in the damage layer	Positron diffusion length L_+ [nm]	Thickness of damaged layer [nm]
C dose 2×10^{14}	0.5034	135	168
C dose 2×10^{15}	0.5081	91	113
N dose 2×10^{14}	0.5103	105	41
N dose 2×10^{15}	0.5115	96	183
Ar dose 2×10^{14}	0.4962	95	38
Ar dose 2×10^{15}	0.5019	108	109

and Ar^+ implantation and noticeable decrease only for C^+ ions, see Table 1. It can be assumed that the concentration of defects created during ion implantation in the damaged layer is increased for higher dose $2*10^{15}$ ions/cm^2 but the distributions of defects are affected slightly by the ion type. For ions like N^+ and Ar^+ the damaged layer thickness firstly increase with the fluence without significant changes of defect concentration, but for C^+ ions only changes of concentration in IL occurs without presence of LRE. Similar observations between ion types are clearly observed for highest dose $2*10^{16}$ ions/cm^2, where larger differences occurs. S-parameter over implantation region falls much faster for N^+ and Ar^+ than C^+ ions. In all cases for highest dose the damaged region drastically increase over the projectile range, which indicate on dependency of LRE on ion fluence.

Schut et al. [25] propose to link the values of S/S_{bulk} to different types of the defects, were S_{bulk} present a value of S parameter for free of defect Si. They observed a similar ratio of about 1.04 for defects formed during irradiation of Si with 30-keV He^+ ions below doses 1×10^{17} He/cm^2 and beyond this dose a ratio 1.10. The first value was assigned as divacancies and the latter one as positrons annihilating at internal surfaces of large cavities. In current studies we get the ratio around 1.05 for two lowest doses and 1.11 for dose $2*10^{16}$ ions/cm^2 in IL. The S- versus W-parameter plot for highest doses in Fig. 4 allow one to distinguish at least two defect types. Two linear dependencies can be noticed. The first one shows increasement of S-parameter to value up to 0.51 ($S/S_{bulk} = 1.05$) and stands for growing divacancies concentration. The second slope is caused by presence of large cavities. This indicate on different types of defects present in the IL than beyond it. The significant difference in S parameter dependence for highest dose could be also caused by amorphization. Wang et al. simulated implantation process for different elements to Si, and observe that over the dose 5×10^{15} C^+ ions/cm^2 the amorphization began [30]. The amorphous regions are shown to give rise to strain in the surrounding crystal lattice

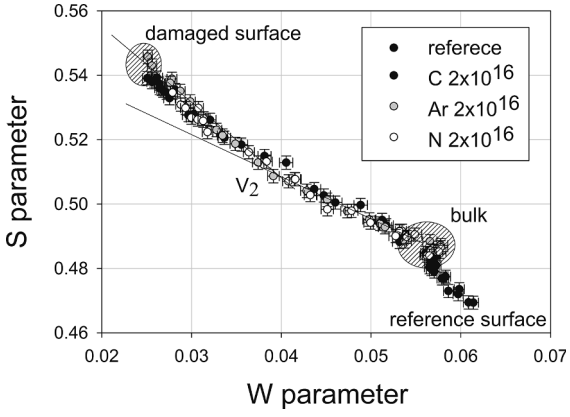

Fig. 4. The annihilation line shape parameters S-W plot for Si samples implanted with C^+, N^+ and Ar^+ ions with energy 25 keV and dose 2×10^{16} ions/cm^2. Two straight lines indicate the presence of two types of defects.

which varies with ion dose in a complicated manner [28]. This accompanied stress could drastically increase number of defects over IL.

The S-parameter dependencies in function of positron incident energy, or its mean depth for different annealing temperatures are shown in Fig. 5. The analysis of these results was done using VEPFIT but now three layer model was assumed. The first layer correspond to the IL. Its thickness, in the fitting procedure according to TRIM calculations (see Fig. 1) was kept constant, i.e., 170 nm for C^+, N^+ and 70 nm for Ar^+-implanted samples. Beyond, the second layer of thickness about 1200 nm was assumed. The third the deepest layer correspond to the substrate bulk region. It is assumed no defects are present there and the diffusion positron length was kept constant, i.e., $L_+ = 230$ nm. The values of the obtained adjustable parameters are presented in Fig. 6 as the function of annealing temperature. Also the defect concentration C_d in $\mu\tau_{bulk}$ unit was calculated using formula:

$$C_d[\mu\tau_{bulk}] = \left(\frac{L_{bulk}}{L_+}\right)^2 - 1 \quad (2)$$

where μ is trapping coefficient for defined type of defect, τ_{bulk} and L_{bulk} is positron lifetime and positron diffusion length in free of defects Si, respectively. During fitting the L_+ value was kept constant equal to 230 nm if it values exceed L_+ of undamaged sample. Its not surprising that the largest changes of S-parameters in the corresponding layers occurs after annealing in 500 °C. According to the literature divacancies in Si can diffuse and disappear at 100–250 °C [27]. Also low-temperature IL regrow below 400 °C was reported [28,29]. These process cause the increase of L_+ in the IL from few to dozens of nanometers, and in case of C^+ irradiated samples also beyond the IL were L_+ increase from 50 to 160 nm. This indicate that recovery process can differ in the IL depending on the type of implanted ion. Its clear that annealing process starts in the most damaged IL but only in case of C^+ ions the removal of defects is observed beyond of it during heating in 500 °C. Further increasing of temperature decrease S-parameter slower and increase positron diffusion length, which is caused by disappearing of the different defects. In the IL the S-parameter and L_+ value is almost stable in temperature range 600–800 °C in the IL, see Fig. 6a. The major changes of S values are then caused mostly by slowly annealing of defects beyond the IL, where changes of these parameters is almost proportional to the temperature. In this layer, after annealing at 800 °C the S-parameter reaches the bulk value. The annealing in 900 °C induces a second significant decrease in the S parameter in IL up to the bulk value. This shows that defects in the IL are more stable, presumably due to the presence of implanted ions and indicate also the presence of LRE in Si implanted with low energetic ions.

4. Conclusion

The defects distribution induced by C^+, N^+ and Ar^+-ion implantation at medium doses (from $2*10^{14}$ to $2*10^{16}$ ions/cm^2, 25 keV) to Si has been investigated by positron beam measurements. Evidence LRE in studied samples was noted for highest dose $2*10^{16}$ ions/cm^2 in all cases. The annealing of samples irradiated with dose $2*10^{16}$ ions/cm^2 shows that recovery process is different in the IL and beyond this layer. The defects start disappear faster in highly damaged part of samples but some of them are stable after annealing at 800 °C. In the IL two characteristic temperatures can be observed standing for annealing of different types of the defects, i.e. lowest temperature 500 °C and 900 °C. Influence of ion type on removal of defects beyond the IL was also noted. The process starts in lower temperature for C^+ than Ar^+ and N^+ ions. The changes of defects concentration beyond the IL are much slower and decrease proportional with temperature in comparison to defect in IL with characteristic annealing steps.

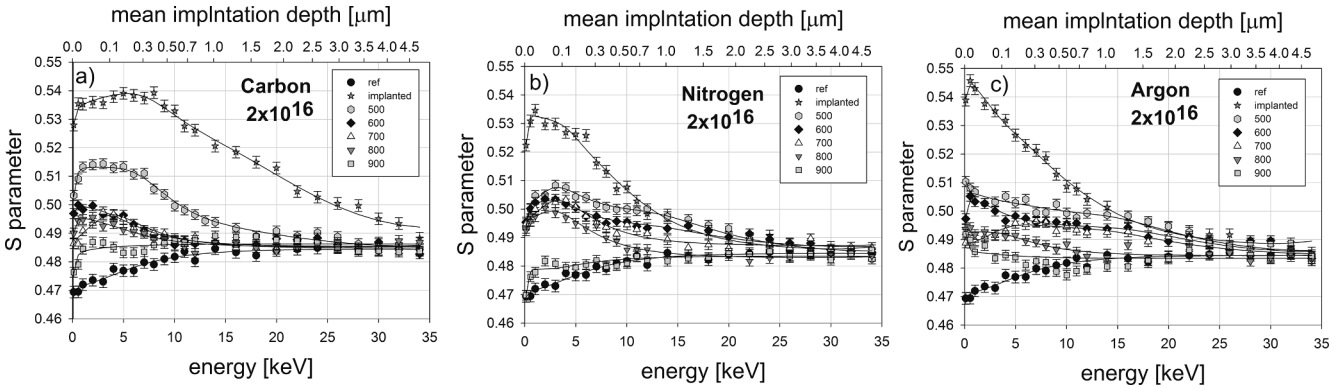

Fig. 5. The S-parameter in function of incident positron energy for Si samples implanted with C^+ a), N^+ b) and Ar^+ c) ions with energy 25 keV and dose 2×10^{16} ions/cm^2 after annealing in temperature regime ranging from 500 to 900 °C. The upper axis correspond to mean implantation depth of positron. The solid lines represent the best fit obtained using VEPFIT code. The values of the adjustable parameters obtained from VEPFIT code are presented in Fig. 6.

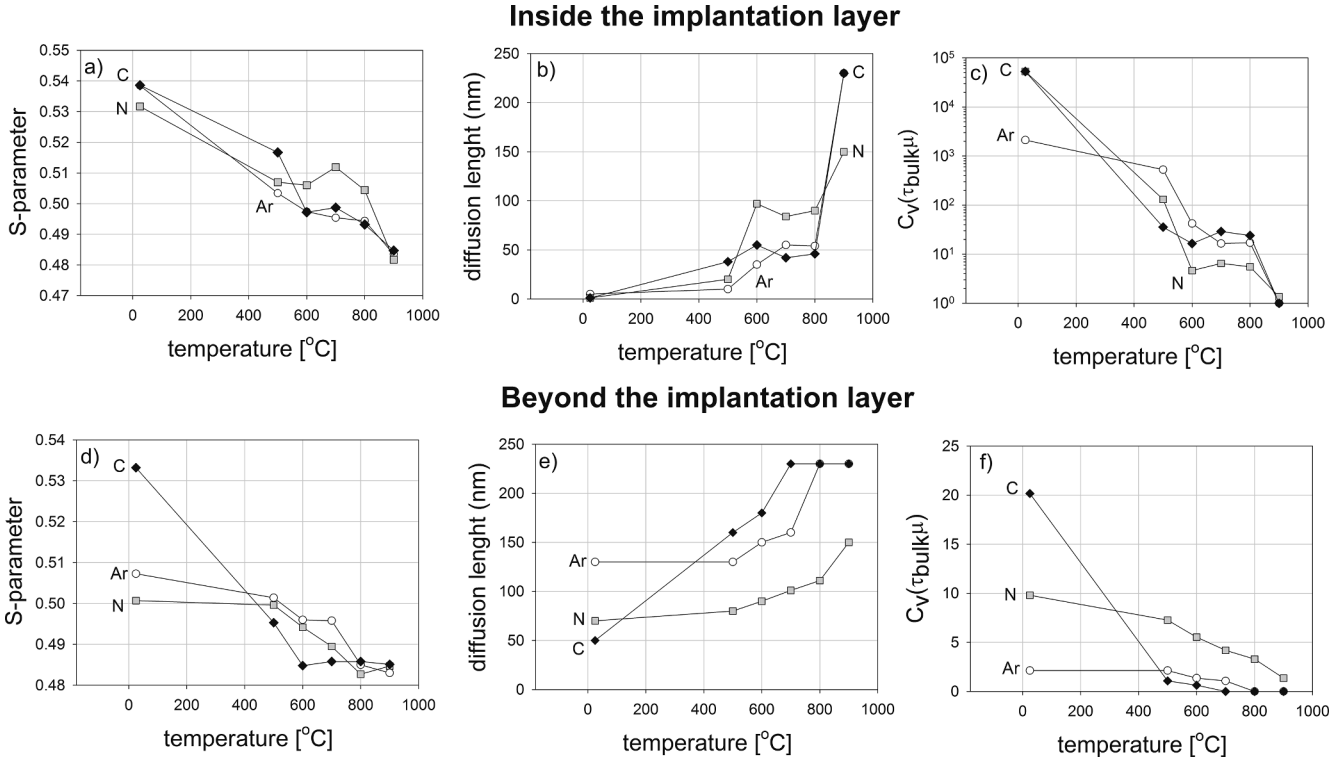

Fig. 6. The fitted values of S-parameter and positron diffusion length L_+ inside (top) and beyond (bottom) implanted layers in function of annealing temperature for Si samples implanted with C, N and Ar ions with energy 25 keV and dose 2×10^{16} ions/cm^2. On plot c) and f) the dependency presenting the defect concentration obtained from adjusted L_+, according Eq. (2) in function of temperature is drawn.

Declaration of Competing Interest

The authors declare that they have no known competing financial interests or personal relationships that could have appeared to influence the work reported in this paper.

References

[1] W.J.M.J. Josquin, Nucl. Instrum. Methods 209 (210) (1983) 581.
[2] P. Werner, S. Eichler, G. Mariani, R. Kögler, W. Skorupa, Appl. Phys. Lett. 70 (1997) 252.
[3] D.D. Berhanuddin, M.A. Lourenço, C. Jeynes, M. Milosavljević, R.M. Gwilliam, K.P. Homewood, J. Appl. Phys. 112 (2012) 103110.
[4] A. Raineri, Battaglia,, E. Rimini, Nucl. Instrum. Meth. Phys. B 96 (1995) 249.
[5] G.S. Was, Fundamentals of radiation damage using ion beam, Springer, New York, 2007.
[6] J.F. Ziegler, Stopping and Ranges of Ions in Matter, 1st ed., Pergamon, New York, 1977.
[7] L. Pelaz, L.A. Marqués, J. Barbolla, J. Appl. Phys. 96 (2004) 5947.
[8] L. Pelaz, L.A. Marqués, M. Aboy, J. Barbolla, G.H. Gilmer, Appl. Phys. Lett. 82 (2003) 2038.
[9] J.W. Corbett, J. Karins, T.Y. Tan, Nucl. Instrum. Methods Phys. Res. 182–183 (1981) 457.
[10] Y. Shi, D.X. Shen, F.M. Wu, K.J. Cheng, J. Appl. Phys. 67 (1990) 1116.
[11] Yu.P. Sharkeev, N.V. Girsova, A.I. Ryabchikov, E.V. Kozlov, O.B. Perevalova, I.G. Brown, X.Y. Yao, Nucl. Instrum. Method. Phys. Res. B 106 (1995) 532.
[12] J. Dryzek, P. Horodek, V.A. Skuratov, Acta Phys. Polon. A 132 (2017) 1585.
[13] J. Dryzek, P. Horodek, M. Dryzek, Appl. Phys. A 124 (2018) 451.
[14] P. Horodek, J. Dryzek, V.A. Skuratov, Vacuum 138 (2017) 15.
[15] P. Horodek, J. Dryzek, Surf. Coat. Technol. 355 (2018) 247.
[16] P. Horodek, Vacuum 164 (2019) 421–427.
[17] P. Hautojdrvi, P. Huttunen, J. Makinen, E. Punkka, A. Vehanen, Mal. Res. Soc. Symp. Proc. 104 (1988) 1.
[18] M. Fujinami, Phys. Rev. B 53 (1996) 13047.
[19] G. Amarenda, G. Venugopal Rao, K.G.M. Nair, B. Visvanathan, Mat. Sci. Forum 255-257 (1997) 650.
[20] S. Eichler, J. Gebauer, F. Börner, A. Polity, R. Krause-Rehberg, E. Wendler, B. Weber, W. Wesch, H. Börner, Phys. Rev. B 56 (1997) 1393.
[21] J. Dryzek, K. Siemek, Appl. Phys. A 125 (2019) 1.

[22] M. Fujinami, T. Miyagoe, T. Sawada, R. Suzuki, T. Ohdaira, T. Akahane, J. Appl. Phys. 95 (2004) 3404.
[23] L.S. Adam, M.E. Law, S. Szpala, P.J. Simpson, D. Lawther, O. Dokumaci, S. Hegde, Appl. Phys. Lett. 79 (2001) 623.
[24] J. Dryzek, P. Horodek, Nucl. Instrum. Meth. B 266 (2008) 4000.
[25] H. Schut, A. van Veen, G.F.A. van de Walle, A.A. van Gorkum, J. Appl. Phys. 70 (1991) 3003.
[26] A. van Veen, H. Schut, J. de Vries, R.A. Hakvoort, M.R. Ypma, A.I.P. Conf, Proc. 218 (1990) 171.
[27] H.J. Stein, F.L. Vook, J.A. Borders, Appl. Phys. Lett. 14 (1969) 328.
[28] O.W. Holland, C.W. White, M.K. El-Ghor, J.D. Budai, J. Appl. Phys. 68 (1990) 2081.
[29] M.K. El-Ghor, O.W. Holland, C.W. White, S.J. Pennycook, J. Mater. Res. 5 (1990) 352.
[30] K.W. Wang, W.G. Spitzer, G.K. Hubler, D.K. Sadana, J. Appl. Phys. 58 (1985) 4553.